Proc. Indian Acad. Sci., Vol. C 2, No. 1, March 1979, pp. 17–27. © Printed in India.

Numerical simulation of monsoon circulations

P K DAS and H S BEDI
Meteorological Office, Lodi Road, New Delhi 110 003

MS received 13 February 1978

Abstract. Short period variations in monsoon rainfall are caused by the westward passage of low pressure systems (depressions) from the northern sector of the Bay of Bengal. A primitive equation model was used to predict the movement of one such depression (20 August 1977). Four research ships from the USSR, which formed a part of the recently concluded Monsoon Experiment, provided additional meteorological data within the field of this depression. This enabled us to fix the depression's initial position with greater accuracy than would have been possible without the ships' data.

The model used a co-ordinate system in which the lower boundary coincided with the earth's surface, while the upper boundary was placed at 200 mb. It resembled a three-dimensional channel with side walls at 0° and 140°E, and northern and southern boundaries at 60°N and the equator. The grid spacing was 250 km. Numerical integration was performed upto 5 days of model time. Gravity waves and other forms of 'noise' were filtered out every 24 hr by a process of adjustment referred to as 'initialisation'. Initialisation after every 24 hr was necessary because the boundary conditions in this regional model did not permit sufficiently rapid dispersal of gravity waves.

In the first experiment only orographic features were included, but the second experiment considered the main features of atmospheric radiation in addition to orography. The paper presents a statement of deviations between the predicted and actual movement of the depression, and discusses reasons for such deviations.

Keywords. Monsoon circulations; numerical simulation; primitive equation model.

1. Introduction

Numerical models help us to understand the different facets of the monsoon. Experiments with models often reveal how the atmosphere is likely to respond to external forces. A recent review of the monsoon by the World Meteorological Organisation (Anon 1976) identified three broad areas where a programme on numerical experimentation could yield valuable results. They are summarised in table 1.

The dimensions of each problem determine whether the numerical model should be global or regional in extent. For a medium-sized computer, it is possible to experiment with regional models of limited geographical extent. But, for some of the problems in table 1, it might well be of advantage to construct a fine-mesh regional model embedded within a global model. The output from the global model could then provide boundary values for the regional model. Such a procedure creates interesting problems in matching the solution at the interface of a fine-mesh nested in a coarser grid.

A list of symbols appears at the end of the paper

Table 1. Scientific aspects of monsoon circulation

1. *Large scale features of the monsoon*
(a) onset of the monsoon
(b) active and break monsoons
(c) heat sources and orographic barriers
2. *Regional aspects*
(a) low level strong cross-equatorial winds off the coast of East Africa
(b) temperature inversions and the planetary boundary layer
(c) monsoon depressions in the Bay of Bengal
(d) convection and heavy rain
(e) mid-tropospheric and equatorial disturbances
3. *Interactions*
(a) interactions between the northern and southern hemisphere
(b) interaction of regional monsoon circulation with:
(i) the central and western Pacific
(ii) mid-latitude waves and
(iii) the circulation in the stratosphere

Numerical experimentation usually follows four different lines of approach. They may be summarised as follows.

1.1. *Predictability experiments*

These are intended to determine to what extent it is possible to forecast the development and movement of pressure systems such as monsoon depressions. In such experiments we need to examine the proper vertical and horizontal resolution for optimum results, and to parameterise clouds and rainfall. An individual cloud is a small entity; its physics cannot be captured in a model which determines the behaviour of the atmosphere over large areas. But, if we consider an ensemble of clouds, it is readily seen that their cumulative effect is not negligible. The process of including such effects, which are individually small but collectively large, is known as parameterisation. Parameterisation of the earth's boundary layer is another important problem in predictability experiments.

1.2. *Controlled numerical experiments*

Experiments in this category are required to determine the relative importance of different meteorological variables, and for specifying their required accuracy. Generally, it is necessary that a numerical model should attain a certain level of stability, before it can be used for control experiments.

1.3. *Observation System Simulation Experiments (OSSE)*

These determine the impact of observations which are irregularly spaced in time and space. Thus, weather satellites, constant-level balloons and other data-collecting devices provide valuable information on meteorological variables, but such data

do not coincide with the other data collected by conventional means. Numerical experiments are needed to devise the most appropriate means of incorporating the additional information.

1.4. *Theoretical model experiments*

Theoretical experiments are designed to explore the major physical processes that lead to changes in weather. Recent experiments have revealed, for example, the impact of soil-reflectivity (albedo) on the rainfall over arid and semi-arid regions of the world. It has been found that sea surface temperature fluctuations could also bring about important changes in the overlying atmospheric circulation. Theoretical experiments often involve numerical integration starting with an idealised atmosphere. In this manner, it is possible to determine the important elements which govern the changes in weather.

A number of numerical models have been devised by national meteorological services in many parts of the world. The governing equations in these models are:

(i) Newton's law of motion relating the acceleration of a moving parcel of air, in a rotating frame, to the forces impressed on it,

(ii) the first law of thermodynamics which equates the rate of change of internal energy to the rate of external heating,

(iii) the principle of conservation of mass, and

(iv) the thermodynamic state of the air.

If the external forces and rate of heating, together with boundary conditions, are properly specified, then it is possible to construct a closed system which can be solved by numerical methods. Usually the system is nonlinear; this makes it necessary to devise special algorithms to ensure computational stability.

But there exist many difficulties which at present are not sufficiently well understood. An example is the effect of very small scale motions upon the large scale motions. For short periods of integration, the small scale motions (known as inertia-gravity waves) may be suppressed because they are more dispersive and contain less energy than the larger scale motions. This is achieved by a process of adjustment, known as ' initialisation ', between the wind and mass, or pressure fields, which are initially in a state of imbalance. Opinions differ on what is the best method of initialisation for a nonlinear system, especially in regional models where the boundary conditions sometimes prevent the rapid dispersal of short-scale motions.

The purpose of the present paper is to use a numerical model to predict the path of an important feature of the monsoon circulation, namely, a monsoon depression in the Bay of Bengal. We used a modified version of a model devised by Shuman & Hovermale (1968). This model has been used by the National Meteorological Centre (NMC) in the USA for several years. Although the model was adopted from Shuman & Hovermale, certain important modifications introduced in the model are described. It is intended to further improve this model so as to study some of the other problems mentioned in table 1. In earlier studies (Das & Bedi 1976, 1977) the model was used to study the mechanical effect of mountains on an idealised monsoon.

The depression selected for this study occurred in the third week of August 1977. This was an interesting situation because additional data were made available by four research ships from the USSR, which took part in a joint Indo-USSR experiment named Monsoon-77. These data enabled us to delineate the location, and the centre of the depression with greater accuracy than would have been possible with the existing network of upper air stations near the northern sector of the Bay of Bengal. Using this data base, it should be possible in future to estimate an optimum network of upper air stations that will be required to improve the prediction of monsoon depressions.

2. Basic equations

The model resembles a three-dimensional rectangular channel. Its northern and southern boundaries were at 60°N and the equator. The two side walls of the model were placed along 0° and 140°E. It had a rigid upper lid at 200 mb, while its lower boundary was treated as a co-ordinate surface coinciding with the earth's surface. For this purpose, σ, a linear function of pressure, was used as the vertical co-ordinate instead of the geometrical height. This has the advantage of simplifying the lower boundary condition, but it is known to create large truncation errors in the vicinity of mountains.

The volume of the channel was divided into four layers to take into account the thermal stratification of the atmosphere. The vertical structure of the model is shown in figure 1. It includes a boundary layer of 50 mb depth adjacent to the earth's surface. The input data consist of geopotentials for 850, 700, 500, 300 and 200 mb, along with the field of sea level pressure. The size of the unit grid was 250 km and variations in the map factor were neglected for simplicity. Unlike Shuman & Hovermale (1968), the model did not have a stratosphere. As we were concerned

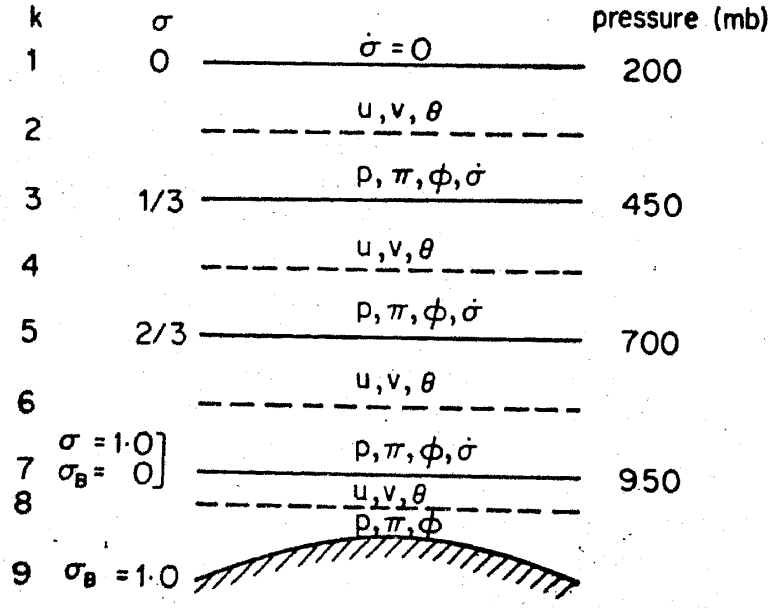

Figure 1. Vertical grid

with a monsoon depression, which is a lower tropospheric phenomenon, this is not a limitation for the present study.

The basic equations of the model are

$$u_t + (uu_x + vu_y + \dot{\sigma}\, u_\sigma) - fv = -\phi_x - C_p\,\theta\pi_x + \mu\nabla^2 u, \tag{1}$$

$$v_t + (uv_x + vv_y + \dot{\sigma}\, v_\sigma) + fu = -\phi_y - C_p\,\theta\pi_y + \mu\nabla^2 v, \tag{2}$$

$$\phi_\sigma + C_p\theta\pi_\sigma = 0, \tag{3}$$

$$\theta_t + (u\theta_x + v\theta_y) + \dot{\sigma}\,\theta_\sigma = \dot{Q}, \tag{4}$$

$$p_{\sigma t} + (u\,p_\sigma)_x + (vp_\sigma)_y + (\dot{\sigma}p_\sigma)_\sigma = 0. \tag{5}$$

On differentiating (5) we have

$$p_\sigma(\dot{\sigma})_{\sigma\sigma} + p_\sigma(u\sigma_x + v\sigma_y) + (u_\sigma\, p_{\sigma x} + v_\sigma p_{\sigma y}) = 0. \tag{6}$$

The system consists of equations (1) and (2) for the rate of change of horizontal momentum, an equation for hydrostatic equilibrium (3), the first law of thermodynamics (4), and the equation of continuity (5). Equation (6) is for the vertical component of motion ($\dot{\sigma}$) in σ co-ordinates and was used to match the solution at the interface of two successive layers of the atmosphere. The different layers are identified by a reference variable k in figure 1. The sigma co-ordinates for the boundary layer are shown by a suffix B in this figure. Thus, $\sigma_B = 0$, 1 refer to the top and bottom of the boundary layer.

When σ is the vertical co-ordinate, there are two terms, instead of one, for the pressure gradient in (1) and (2). Near steep mountains, where there are large pressure gradients, these two terms are individually large but of opposite sign. Consequently, the determination of x and y derivatives in the first two terms on the right of (1) and (2) often provides a wrong representation of the pressure gradient. A method of minimising this error will be discussed shortly.

A non-staggered horizontal grid, with a scheme for averaging and differencing the dependent variables, was used for computing partial derivatives in the model equations. This scheme is not strictly energy-conserving and does not handle short scale waves very well, but it is satisfactory for short range prediction. As boundary conditions, the vertical velocity ($\dot{\sigma}$) was made to vanish at the top and bottom of the model atmosphere. We have

$$\dot{\sigma} = 0 \quad \text{at} \quad \sigma = 0 \quad \text{and} \quad \sigma_B = 1{\cdot}0.$$

It may be noted that if pressure was used as the vertical co-ordinate, the boundary condition at the surface would be

$$\omega_s = \frac{\partial p_s}{\partial t} + \mathbf{V}_s \cdot \nabla\, p_s.$$

Apart from difficulties in determining the appropriate value of V_S, another difficulty would arise. During the course of integration the surface pressure (p_s) would change, and there was no way of knowing whether ω_s was being determined at the same grid points throughout the integration. Such difficulties are avoided by the sigma system.

Along the lateral walls, the time derivatives of all dependent variables were made to vanish. We put

$$u_t = v_t = 0;$$

$$p_{\sigma t} = \theta_t = 0; \qquad X = 0, \quad 140°\text{E}; \quad Y = 0, \; 60°\text{N}. \tag{7}$$

Physically this implies a rigid wall along the sides. This has the effect of reflecting inertia-gravity waves, and preventing their outward dispersal from the region. We intend to experiment with more realistic boundary conditions in later studies, but for the present these boundary conditions were retained because of their simplicity and the limitations imposed by a small computer memory.

3. Initialisation

In integrating primitive equation models, it is necessary to remove, as much as possible, sources of inertia-gravity waves from the initial data. This is achieved by minimising the divergence in the initial wind and pressure fields. Although there exist several techniques which may be applied, there is no general method for low latitudes. This difficulty arises because the process of geostrophic adjustment is not well understood for the tropics. Specifically, it is not known whether the pressure adjusts to the wind, or the other way round in low latitudes. For our purpose, we carried out a scheme of forward integration for 1 hr followed by backward integration for another hour. One half the initial pressure and height fields were restored at the end of each cycle, while the wind field was allowed to adjust itself to the pressure freely. The factor $\frac{1}{2}$ was chosen on empirical considerations, so as to provide some allowance to the pressure to adjust to the wind at the end of each cycle. If the full pressure and height fields were restored, it would force the wind to adjust to the pressure. But, as we have noted, the process of adjustment is not known in low latitudes; consequently, an empirical procedure was adopted. The diffusion and heating terms were not included during initialisation because they represent irreversible processes.

We found it necessary to repeat initialisation after every 24 hr to suppress the growth of inertia-gravity waves. This is a limitation of the model, but is probably caused by the boundary conditions at the lateral walls.

4. Inclusion of high mountains

The inclusion of high mountains in regional models is difficult because of large truncation errors. Very little is known about the inertia-gravity waves that are generated by such barriers. But, as the path of monsoon depressions is influenced by mountain ranges, we included their effect in our model.

Truncation errors near smoothed mountain profiles were reduced by removing the hydrostatic component of the geostrophic field. The residual geopotential is then considered to be the dependent variable. As the new variables are now much smaller than the previous ones, their gradients are also reduced.

We define

$$\phi'(x, y, p, t) = \phi(x, y, p, t) - \bar{\phi}(p), \tag{8}$$

$$\theta'(x, y, p, t) = \theta(x, y, p, t) - \bar{\theta}, \tag{9}$$

where $\bar{\phi}(p)$ is the mean geopotential for a surface of constant pressure. A mean potential temperature for the region is similarly defined by

$$\bar{\theta} = [\langle\phi_T\rangle - \langle\phi_S\rangle] \div [C_p(\langle\pi_S\rangle - \pi_T)]. \tag{10}$$

The subscripts T and S refer to values at 200 mb and the earth's surface, and $\langle\ \rangle$ denotes an average value. Thus, $\langle\phi_S\rangle$ is the mean surface geopotential and

$$\bar{\phi}(p) = [\langle\phi_S\rangle(\pi - \pi_T) - \langle\phi_T\rangle(\langle\pi_S\rangle - \pi)] \div [\langle\pi_S\rangle - \pi_T]. \tag{11}$$

It may be noted that (11) is derived by integrating the hydrostatic equation

$$\frac{\partial\phi}{\partial\pi} = -C_p\theta,$$

and assuming a constant value of $\bar{\theta}$ given by (10). The effect is thus to introduce a ' reference ' atmosphere, which in this case is defined by (10) and (11). It would be interesting to experiment with other types of ' reference ' atmospheres. This will be reported in a later study.

Introducing (8) and (9) on the right side of (1) and (2) we have

$$\nabla_\sigma\phi - C_p\theta\nabla_\sigma\pi = \nabla_\sigma\phi' - C_p\theta'\nabla_\sigma\pi. \tag{12}$$

From contours of the topographic features, we computed the sea level pressure (p_S) by assuming hydrostatic balance. Thus,

$$\phi_S - \phi_0 = R\bar{T}_S \ln(p_S/p_0), \tag{13}$$

where $p_0 = 1000$ mb, ϕ_0 is the geopotential corresponding to p_0 and $\bar{T}_S$ is a mean temperature between sea level and the height of the barrier. Deviations (ϕ') from the mean geopotential field were next computed by (8) and (9) for different surfaces of constant pressure. Subsequently, the appropriate value of ϕ' for a given sigma surface was obtained by Lagrange's interpolation. This expresses ϕ' by the polynomial

$$\phi' = \sum_{k=1}^{5} L_k(p)(\phi')_k, \tag{14}$$

where the index k refers to values of ϕ' on different pressure surfaces, and

$$L_k(p) = \frac{(p-p_S)\,(p-850)\,\ldots\,(p-200)}{(p_k-p_S)\,(p_k-850)\,\ldots\,(p_k-200)}\,. \tag{15}$$

It was observed that the combination of (12) and (15) considerably reduced truncation errors. If we used the original geopotential field, with hydrostatic interpolation to obtain the value of ϕ for a sigma surface, then an abnormal anticyclone was generated over the Himalayas.

5. Non-adiabatic heat input

A depression is accompanied by rainfall. This provides an important source of non-adiabatic heating (referred to as ' diabatic ' heating), because of the latent heat released by condensation of water vapour. Unfortunately, it was not possible to incorporate this important heat source in the model because of constraints on computer memory. Although, the present model represents a ' dry ' atmosphere, we included (a) incoming solar radiation, (b) the albedo or reflectivity of the earth's surface, (c) long wave radiation received from the atmosphere and also emitted by the earth, and (d) the flux of sensible heat from the earth. Thus, $\dot{Q}$, the rate of diabatic heating in (4), is

$$\dot{Q} = \dot{Q}_1 + \dot{Q}_2, \tag{16}$$

where
$$\dot{Q}_1 = \int [Q_0\,(1-\alpha) + \epsilon\,\sigma_S\,T_a^4\,(a+b\sqrt{e}) - \epsilon\sigma_S\,T_e^4 + 4\epsilon\sigma_S\,T_a^3\,(T_e-T_a)]\,\sigma d\sigma, \tag{17}$$

$$\dot{Q}_2 = \frac{\partial}{\partial Z}\left(K_\theta\,\frac{\partial\theta}{\partial Z}\right). \tag{18}$$

Expression (17) indicates that the rate of heat absorbed by a column of air near the earth ($\dot{Q}$) is made up of (a) the total flux of heat on a horizontal surface less the amount reflected by the soil, (b) the infra-red radiation from the atmosphere absorbed at the ground (long wave counter radiation), (c) the infra-red radiation emitted by the earth, and (d) a correction term because of the difference in temperature between the earth's surface (T_e) and of the adjacent air (T_a) (Sellers 1965). The second term in (17) for the long wave counter radiation included a contribution by the water vapour in the planetary boundary layer. Appropriate values of the surface albedo were used in the model. For Q_0 we took the values reported by Ramachandran and Kelkar (1977). The different components of $\dot{Q}_1$ are integrated from the surface of the earth ($\sigma_B = 1{\cdot}0$) to the top of the planetary boundary layer ($\sigma_B = 0$) in the model. The second component of diabatic heating is the flux of sensible heat from the surface. This has been parameterised in terms of a thermal eddy-diffusivity, which is treated as a constant for simplicity.

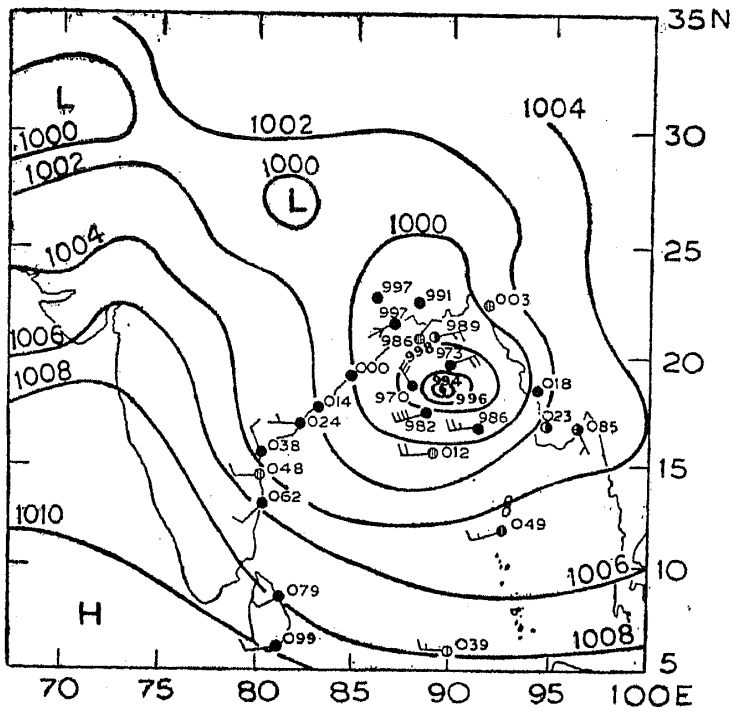

Figure 2. Initial position of depression (20 August 1977)

6. Results

Two experiments were performed with this model. In the first, only the mountains were included, while the second included the mountains as well as diabatic heating. Figure 2 shows the initial position of the depression on 20 August 1977. It will be observed that the additional wind data provided by research vessels from the USSR helped to locate the centre of the depression with more precision than would have been otherwise possible.

In the first experiment it was found possible to integrate the model upto 5 days, but the second experiment had to be terminated after 2 days because of the rapid growth of inertia-gravity waves. The growth of such waves may be monitored by recording the variation of r.m.s. values of the pressure tendency. This was done, and the results are shown in figure 3. The figure depicts a jump every 24 hr, because the mass and wind fields were initialised every 24 hr to suppress inertia-gravity waves. Figure 4 shows the observed and predicted track of the depression. There is a discrepancy of approximately 250 km in the observed and predicted landfall of the depression, if no heating is included, but the preliminary results indicate an improvement when heating is included. As mentioned earlier, we were unable to include the release of latent heat by condensation of water vapour. This clearly needs consideration in future experiments. We observe that in the absence of heating, successive initialisation after every 24 hr leads to an approximate steady state after 5 days, but this is not the case when diabatic heating is included. It appears that there is no decrease in the amplitude of such waves even after an initial rise between 24 and 48 hr, when diabatic heating is put in the model. It is known that interia-gravity waves are more dispersive than the meteorologically important Rossby waves, and they contain less

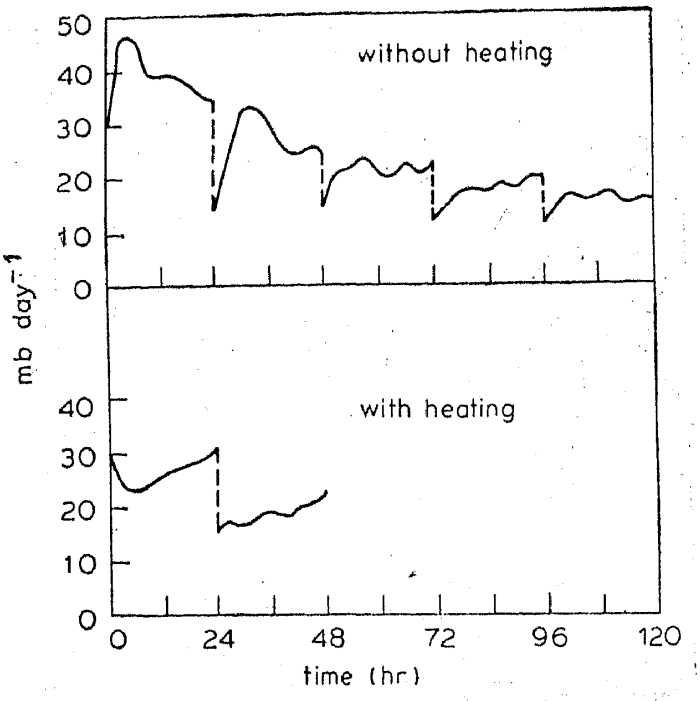

Figure 3. Variation of root mean square of pressure tendency ($p_{\sigma t}$)

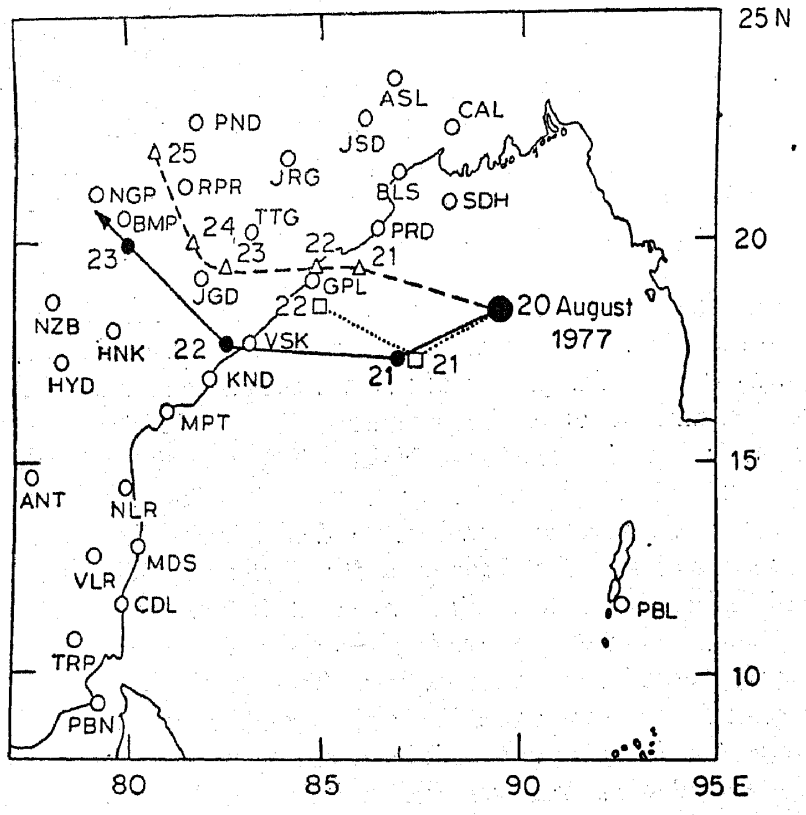

Figure 4. Observed and predicted tracks. Observed tracks are shown by a dashed line with triangles. The predicted track, without heating, is shown by a firm line, The predicted track with heating is shown by a dotted line.

energy than Rossby waves. But, it is not known how much of the energy of Rossby waves is extracted by interactions between Rossby waves and inertia-gravity waves. We wish to examine this aspect in another paper.

List of symbols

The following are the symbols not explicitly defined in the text.

a, b	constants ($a = 0{\cdot}605$, $b = 0{\cdot}048$)
C_p	specific heat at constant pressure
e	vapour pressure (17·3 mb)
k	R/C_p, where R is the gas constant
k_θ	eddy coefficient of thermal diffusivity (10^4 cm^2 s^{-1})
p	atmospheric pressure
p_s	surface pressure
$\dot{Q}$	rate of non-adiabatic heating per unit mass
$\dot{Q}_1$	net radiative heating due to incoming solar radiation, and outgoing long wave radiation
$\dot{Q}_2$	flux of sensible heat transfer from the earth's surface
T_a	air temperature 25 mb above the earth's surface
T_e	temperature at the earth's surface
u, v	zonal and meridional components of the vector wind in Cartesian co-ordinates (oxy), with the x and y axes pointing to the east and the north
α	albedo or reflectivity of the earth's surface
ϵ	surface emissivity (0·9)
θ	potential temperature (°K)
μ	eddy diffusivity (10^5 m^2 s^{-1})
π	$(p/1000)^k$
σ	vertical co-ordinate $\sigma = (p - 200)/p_S - 200)$
σ_S	Stefan-Boltzmann constant ($8{\cdot}14 \times 10^{-11}$ ly min^{-1} °K^{-4})
ϕ	geopotential (m^2 s^{-1})

References

Anon 1976 *The monsoon experiment*, World Meteorological Organisation, Geneva, GARP Publications Series No. 18, pp. 123

Das P K & Bedi H S 1976 *Proc. Symp. Tropical Monsoons*, Indian Institute of Tropical Meteorology, Pune, pp. 51-58

Das P K & Bedi H S 1977 *Indian J. Met. Hyd. Geophys.* **29** 375

Phillips N A 1974 National Meteorological Centre Technical Note No. 104, Washington, pp. 40

Ramachandran S & Kelkar R R 1977 *Indian J. Meterorol. Hyd. Geophys.* **28** 81

Sellers W 1965 *Physical climatology* (University of Chicago Press) pp. 272

Shuman F G & Hovermale J B 1968 *J. Appl. Met.* **7** 525